


Sacrificial photocatalysis: removal of nitrate and hydrogen production by nano-copper-loaded P25 titania. A kinetic and ecotoxicological assessment

Roberta Lucchetti¹ · Antonietta Siciliano² · Laura Clarizia¹ · Danilo Russo¹ ·
Ilaria Di Somma³ · Francesco Di Natale¹ · Marco Guida² · Roberto Andreozzi¹ ·
Raffaele Marotta¹ 

Received: 7 October 2016 / Accepted: 19 December 2016 / Published online: 7 January 2017
© Springer-Verlag Berlin Heidelberg 2017

Abstract The photocatalytic removal of nitrate with simultaneous hydrogen generation was demonstrated using zero-valent nano-copper-modified titania (P25) as photocatalyst in the presence of UV-A-Vis radiation. Glycerol, a by-product in biodiesel production, was chosen as a hole scavenger. Under the adopted experimental conditions, a nitrate removal efficiency up to 100% and a simultaneous hydrogen production up to 14 $\mu\text{mol/L}$ of H_2 were achieved (catalyst load = 150 mg/L, initial concentration of nitrate = 50 mg/L, initial concentration of glycerol = 0.8 mol/L). The reaction rates were independent of the starting glycerol concentration. This process allows accomplishing nitrate removal, with the additional benefit of producing hydrogen under artificial UV-A radiation. A kinetic model was also developed and it may represent a benchmark for a detailed understanding of the process kinetics. A set of acute and chronic bioassays (*Vibrio fischeri*, *Raphidocelis subcapitata*, and *Daphnia magna*) was performed to evaluate the potential ecotoxicity

of the nitrate/by-product mixture formed during the photocatalytic process. The ecotoxicological assessment indicated an ecotoxic effect of oxidation intermediates and by-products produced during the process.

Keywords Nitrate removal · Hydrogen production · Photoreforming · Sacrificial photocatalysis · Glycerol · Ecotoxicity

Introduction

Nitrate is one of the most abundant and widespread environmental contaminants, due to the massive introduction of nitrogen to ground and surface waters, as a result of agricultural activities and disposal in the environment of livestock manure (Rao and Puttanna 2000). High concentrations of nitrate in natural waters can affect human health and cause methemoglobinemia, also known as “blue baby” syndrome, a fatal disease in early infancy (Knobeloch et al. 2000). Nitrate can be endogenously transformed into nitrite by the digestive bacterial microflora; nitrite ions can be subsequently transformed into *N*-nitroso compounds, which are highly mutagenic molecules (Ward et al. 2005). Camargo and Ward (1995) indicated that nitrate ecotoxicity to aquatic animals increases with increasing exposure time and nitrate concentration, due to the conversion of oxygen carriers (e.g., hemoglobin, hemocyanin) to species that are unable to deliver oxygen (e.g., methemoglobin).

Biological processes are widespread for nitrate removal from civil wastewater. Despite this, chemical–physical processes are preferred over biological processes in many industrial applications. Electro-kinetic denitrification,

Responsible editor: Suresh Pillai

✉ Marco Guida
marco.guida@unina.it

✉ Raffaele Marotta
rmarotta@unina.it

¹ Dipartimento di Ingegneria Chimica, dei Materiali e della Produzione Industriale, Università di Napoli “Federico II”, P.le V. Tecchio 80, 80125 Naples, Italy

² Dipartimento di Biologia, Università di Napoli “Federico II”, via Cinthia ed. 7, 80126 Naples, Italy

³ Istituto di Ricerche sulla Combustione, Centro Nazionale delle Ricerche IRC-CNR, p.le V. Tecchio 80, 80125 Naples, Italy

reverse osmosis, ion exchange, and chemical reduction are efficient options. In spite of their effectiveness, both biological and chemical-physical processes have some drawbacks, such as sludge production, relatively high operative costs, and formation of toxic by-products (Kapoor and Viraraghavan 1997).

Among novel technologies for nitrate removal from wastewaters, photocatalytic reduction processes could allow solar energy to convert nitrate to less harmful by-products, such as nitrogen. During the last decade, numerous studies focused on TiO₂ materials doped with noble metals added in order to increase the photocatalytic activity of pristine TiO₂ catalysts (Li et al. 2010; Anderson 2011; Kominami et al. 2001; Soares et al. 2014; Wehbe et al. 2009; Gao et al. 2004; Zhang et al. 2005; Yang et al. 2013; Doudrick et al. 2013; Parastar et al. 2013; Ren et al. 2015). The photocatalytic reduction of nitrate is generally performed under deaerated conditions and in the presence of organic compounds. The organic compounds act as scavengers of photogenerated holes, thus reducing the parasitic recombination of photogenerated electron hole (sacrificial photocatalysis). However, there are only few literature studies focused on the use of TiO₂-based materials doped with copper, a metal cheaper than the noble metals, such as Ag, Au, Pd, and Pt, for removing nitrate from wastewater (Luiz et al. 2012; Yamauchi et al. 2011; Jin et al. 2004; Sá et al. 2009). According to recent literature findings (Colon 2016; Puga 2016), some selected photocatalytic systems for nitrate removal from wastewaters can also produce hydrogen. Recently, Clarizia et al. (2016a, 2016b) demonstrated that hydrogen production rate could be enhanced with respect to bare P25 through photocatalytic reforming of oxygenated species (i.e. alcohols and carboxylic acids) in the presence of copper nanoparticles “in situ” photodeposited on P25 catalyst. Analytical investigations showed the formation on TiO₂ of zero-valent copper nanoparticles with a mean diameter close to 30 nm. The aim of the present study is to demonstrate the possibility of using the same catalyst (nano-Cu_(s)/P25) for nitrate removal from aqueous solution and hydrogen generation under artificial UV-A-Vis radiation. Glycerol, a major by-product in biodiesel manufacturing processes (Tan et al. 2013), was chosen as a model hole scavenger (Taylor et al. 2014; Jung et al. 2016), although many other species such as alcohols, sugars, and carboxylic acids may be considered in the applications (Yoong et al. 2009). Moreover, the presence of these species in nitrate-containing wastewater may be hypothesized.

A multilevel ecotoxicological study was carried out in order to evaluate the ecotoxicity of treated and untreated solutions. A battery of acute and chronic ecotoxicity tests, adopting biological models belonging to various trophic levels such as *Vibrio fischeri* (bacteria), *Raphidocelis subcapitata* (green algae), and *Daphnia magna* (crustacean), was thus performed.

Material and methods

Materials

Glycerol ($\geq 99.5\%$), TiO₂ nanopowder (aeroxide TiO₂-P25), cupric sulfate pentahydrate (CuSO₄·5H₂O, $>98\%$), sodium nitrate ($>99\%$), sodium nitrite (99%), ammonium chloride (99.5%), phenol ($>99\%$), ethanol ($>99\%$), sodium nitroprusside dihydrate, sodium hypochlorite, and sodium citrate tribasic ($>99\%$) were purchased from Sigma-Aldrich. Bidistilled water was used for the preparation of the suspensions.

Test organisms *V. fischeri* and reagents for ecotoxicity assessment (i.e., OAS, osmotic adjusting solution of sodium chloride, 22%) were supplied by ECOTOX LDS.

Photocatalytic device

Photocatalytic experiments were carried out in an annular glass batch reactor (310 mL). The reactor was magnetically stirred and thermostated at 25 °C through a thermostatic bath (Falc GTR 90). A high-pressure mercury vapor lamp (Helios Italquartz, 125 W), mainly emitting in the wavelength range of 300–400 nm (manufacturer’s data), was placed in the center of the photoreactor. On the top of the photoreactor, an inlet allowed feeding reactants and nitrogen gas and an outlet was used to collect liquid/gaseous samples at varying reaction times. The photon fluxes of the Hg-lamp were 210 W/m² for the wavelength range 300–400 nm and 135 W/m² for wavelengths higher than 400 nm.

Preparation of nano-Cu-loaded TiO₂ (nano-Cu₍₀₎/P25)

Commercial TiO₂-P25 particles were used with no surface modifications or pretreatments. For each run, a fixed amount (45 mg) of bare titania dioxide (P25) was initially added to the aqueous mixture (300 mL) containing glycerol at a desired concentration; the pH of the mixture was not adjusted. With the aim of avoiding the reaction between dissolved oxygen and photoelectrons, the device was purged with nitrogen at a flow rate of 0.3 L/min for 30 min before adding of cupric sulfate pentahydrate to the slurry mixture. The initial cupric ion concentration ([Cu(II)]₀ = 0.24 mM) was chosen on the basis of previous literature results on the kinetic modeling of hydrogen production through photocatalytic reforming of glycerol (Clarizia et al. 2016). In particular, a percentage of 10% (w/w) of copper was initially added into the mixture (150 mg/L, titania). The deposition of copper on TiO₂ was realized by switching on the lamp and irradiating the suspension up to the complete reduction of cupric ions, which was monitored by sampling at different time intervals. Once prepared, the catalyst was characterized following procedures reported elsewhere (Clarizia et al. 2016b). The catalyst resulted to be constituted of zero-valent copper nanoparticles

deposited on TiO₂ surface. The main properties of the photocatalyst (nano-Cu₀/P25) are listed in Table 1.

Analytical procedures

Sodium nitrate was added as nitrogen source when cupric ions were completely photoreduced on the P25 titania surface (1 h after adding CuSO₄·5H₂O). In some experiments, sodium nitrite or ammonium chloride were used. Throughout the photocatalytic runs, the system was kept under an inert atmosphere (nitrogen) in order to prevent the entrance of air in the photoreactor.

Gaseous and liquid samples were collected at various treatment times by means of Tedlar gas sampling bags (1 L) and glass syringes (10 mL), respectively. Gaseous samples were analyzed by a gas-chromatograph (Agilent 7820A) equipped with a HP-PLOT Molesieve 5A column (Agilent) and a TCD detector using argon as carrier gas. After being filtered on regenerated cellulose filters (pore diameter 0.20 μm, Scharlau), the liquid samples were used to measure pH and concentrations of total dissolved copper, nitrate, nitrite, and ammonia.

The concentration of total dissolved copper was measured by a colorimetric method using an analytical kit (Macherey-Nagel) based on the oxalic acid bis-cyclohexylidenehydrazide (cuprizone). An UV-Vis spectrophotometer (Cary 100 UV-Vis Agilent) was used for colorimetric analysis at 585 nm. Nitrate and nitrite were analyzed using ion chromatography (883 Basic IC PLUS, Metrohm) with a Metrosep A Supp 5250/4 column (eluent: 3.2 mmol/L sodium carbonate, 1.0 mmol/L sodium hydrogen carbonate). Ammonia concentration was measured using a colorimetric method (indophenol blue method). The pH of the solution was monitored by means of an Orion 420 p pH-meter (Thermo). The photon flux of the lamp was measured through a digital radiometer (Delta Ohm HD 2102.1).

Ecotoxicological procedures

Test organisms were exposed to aqueous filtered samples, collected at various treatment times (0, 90, 180, and 360 min), and diluted 1/10. At the same time, negative control tests were carried on tested species with bidistilled water and with a solution containing only nano-Cu₀/P25.

Table 1 Properties of the nano-Cu₀/P25 photocatalyst (Clarizia et al. 2016b)

Support	Commercial grade, aerioxide TiO ₂ -P25
Anatase/rutile ratio	80/20
BET-specific surface area (m ² /g)	50 ± 15
Average primary TiO ₂ particle size (nm)	21
Nature of copper deposited	Zero-valent copper
Average primary Cu particle size (nm)	30
Band gap (eV)	2.6

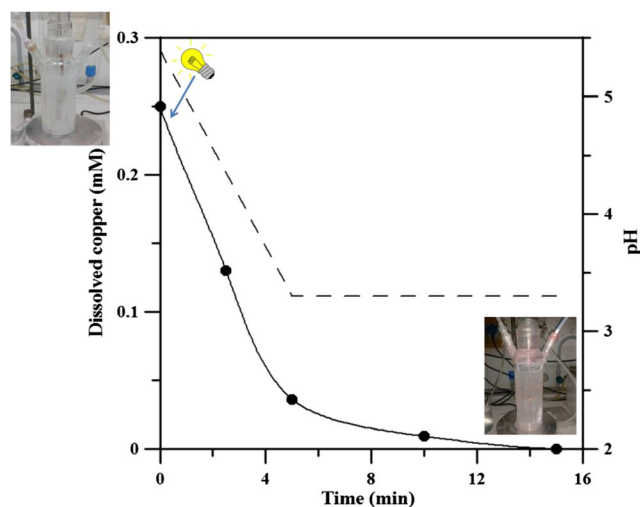


Fig. 1 Dissolved copper photoreduction (continuous line) and pH (dashed line) profiles. C_{in} (P25) = 150 mg/L, Cu/TiO₂ ratio: 10% w/w. Hole scavenger agent: glycerol (0.8 mol/L)

Acute Microtox tests were performed using *V. fischeri* NRRL-B-11177 (Gram-negative marine bioluminescent bacteria). The ISO 11348-3 protocol (ISO 11348-3: 2008) was followed using a Microtox Model 500 luminometer. This protocol allowed the measurement of light outputs at 490 nm with readings at varying exposure times (5 and 15 min) and a temperature of 15 °C.

As an endpoint for the acute ecotoxicity tests, the inhibition of luminescence naturally emitted by the bacterium was used. Tests were carried out at least in triplicate with a control solution. The data were statistically processed by the instrument software and the result was expressed as percentage of luminescence inhibition (% I).

Chronic toxicity growth inhibition tests with unicellular algae on *R. subcapitata* were performed following ISO 8692 protocol (ISO 8692: 2012). The growth of the algae exposed to the sample was compared to the growth of the algae in a negative control. The algal density was determined by an indirect procedure using a spectrophotometer (Hach Lange DR5000) equipped with a holder for 5-cm cells. The specific growth rate of *R. subcapitata* in each replicate culture was calculated from the logarithmic increase in cell density in the range 0–72 h using Eq. (1):

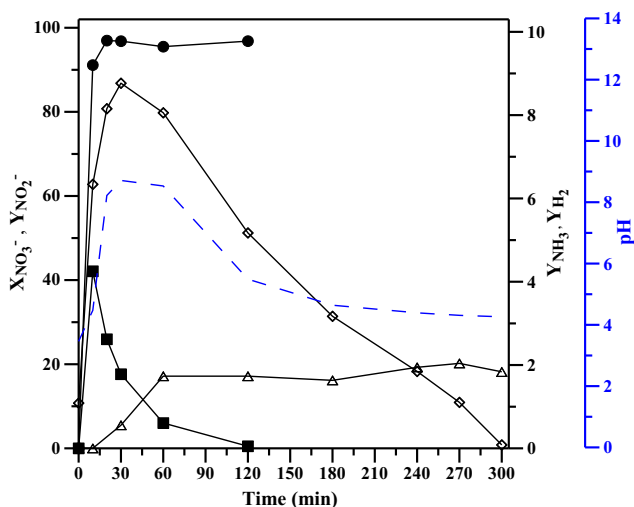


Fig. 2 Nitrate photocatalytic reduction: $[Cu(II)]_0 = 0.24$ mmol/L; C_{in} (P25) = 150 mg/L; C_{in} (NO_3^-) = 50 mg/L; (glycerol) $_0 = 0.8$ mol/L. Conversion degree (%): nitrate (black circle). Yields (%): nitrite (black square), hydrogen (white triangle), ammonia (white diamond). pH (broken line)

$$\psi = \frac{\ln N_n - \ln N_0}{t_n - t_0} \quad (1)$$

Fig. 3 Effect of hole scavenger concentration. $[Cu(II)]_0 = 0.24$ mmol/L; C_{in} (P25) = 150 mg/L; C_{in} (NO_3^-) = 50 mg/L; (glycerol) $_0$: 0.8 mol/L (black circle), 8.0×10^{-2} mol/L (black square), 8.0×10^{-3} mol/L (black triangle), and 8.0×10^{-4} mol/L (black diamond). **a** Nitrate conversion degree. **b** Nitrite yield. **c** Hydrogen concentration. **d** pH

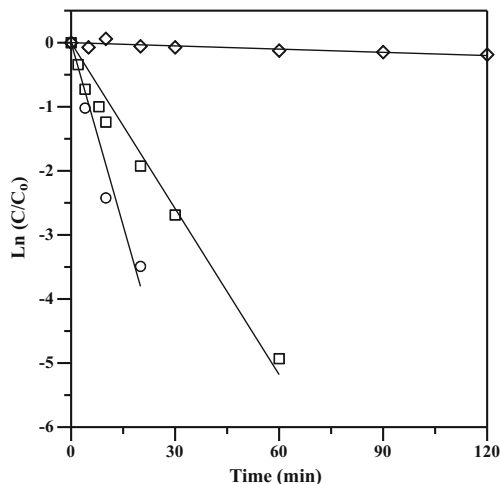
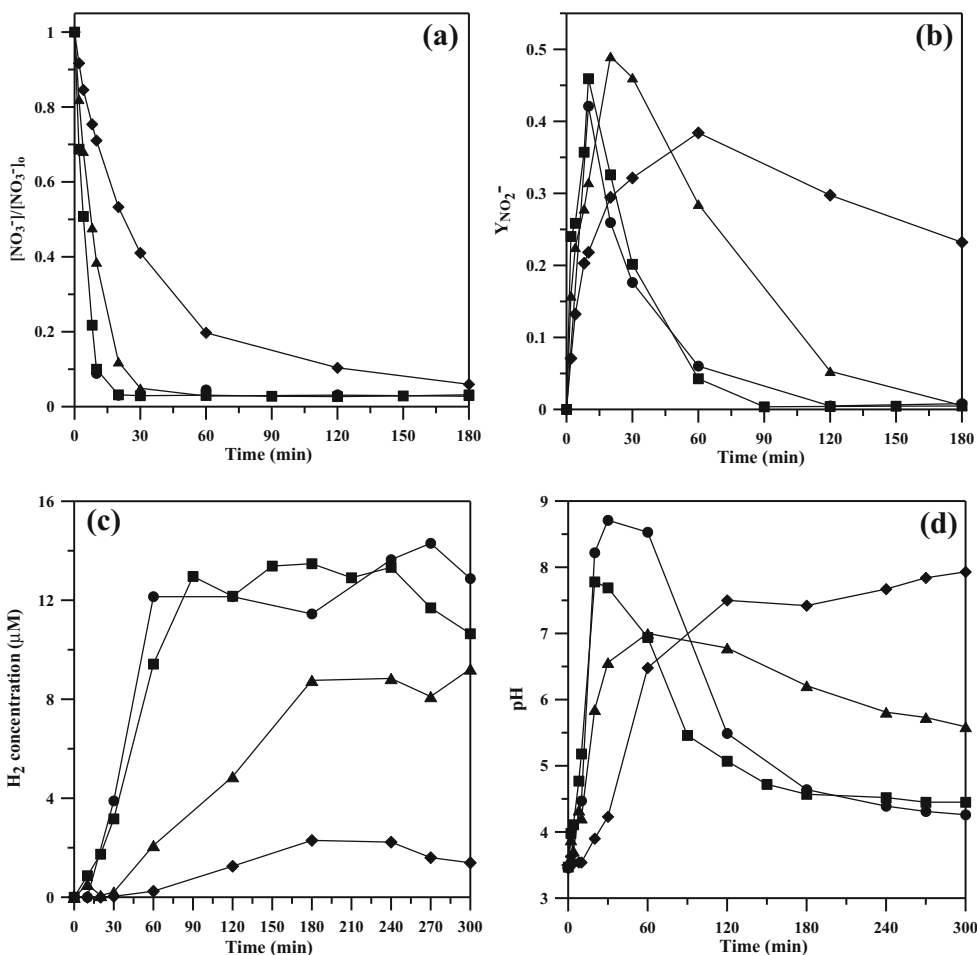
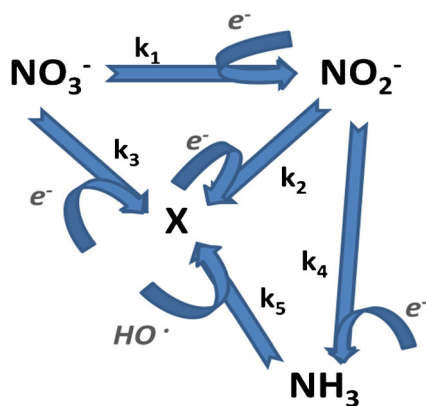


Fig. 4 Pseudo-first-order kinetics for nitrate, nitrite, and ammonia removal versus reaction time; $C_o = 50$ mg/L, $[Cu(II)]_0 = 0.24$ mmol/L; C_{in} (P25) = 150 mg/L; (glycerol) $_0 = 0.8$ mol/L. Nitrate (white circle), nitrite (white square), and ammonia (white diamond)

In Eq. (1), N_0 is the cell concentration at $t = 0$, N_n the final cell concentration after 72 h of exposure, t_0 is the start time of measurement, and t_n is the time of last



Scheme 1

measurement (hours from the start). The percentage inhibition of cell growth was calculated as the difference between the rate growth of the control and the rate growth of the sample and expressed as the mean (\pm standard deviation) of the replicates for $p \leq 0.05$.

$\text{CaCl}_2 \cdot 2\text{H}_2\text{O}$ (18 mg/L), $\text{MgSO}_4 \cdot 7\text{H}_2\text{O}$ (15 mg/L), NH_4Cl (15 mg/L), $\text{MgCl}_2 \cdot 6\text{H}_2\text{O}$ (12 mg/L), KH_2PO_4 (1.6 mg/L), $\text{FeCl}_3 \cdot 6\text{H}_2\text{O}$ (0.08 mg/L), $\text{Na}_2\text{EDTA} \cdot 2\text{H}_2\text{O}$ (0.1 mg/L), H_3BO_3 (0.185 mg/L), $\text{MnCl}_2 \cdot 4\text{H}_2\text{O}$ (0.415 mg/L), ZnCl_2 (3.0×10^{-3} mg/L), $\text{CoCl}_2 \cdot 6\text{H}_2\text{O}$ (1.5×10^{-3} mg/L), $\text{Na}_2\text{MoO}_4 \cdot 2\text{H}_2\text{O}$ (7.0×10^{-3} mg/L), and $\text{CuCl}_2 \cdot 2\text{H}_2\text{O}$ (1.0×10^{-5} mg/L) salts were used for the preparation of algal test medium.

The effect of the solution exposure on the reproductive and survival outputs was assessed in a semi-static chronic test according to the standard protocol for the *Daphnia magna* Reproduction Test (ISO 6341: 2012).

Larval daphnids were exposed for a period of 21 days to untreated and treated solutions. For each sample, 10 beakers each containing a test solution and a single test organism were prepared. The solutions were renewed three times weekly and daphnids were fed daily with a feeding rate of 3.0×10^7 algal cells per animal per day. Survival and offspring production were daily recorded; pH and oxygen were measured too. Test beakers were incubated at 21 ± 1 °C under a photoperiod of 12-h light and 12-h dark.

Reconstituted water was used as dilution water for cladoceran toxicity tests (CaCl_2 dihydrate 290 mg/L, MgSO_4 heptahydrate 120 mg/L, NaHCO_3 65 mg/L, and KCl 6 mg/L with a pH of 7.8 ± 0.2).

Results and discussion

Figure 1 shows the profile of dissolved copper concentration and pH during the photoreductive deposition of cupric ions on P25.

As shown in the photos of Fig. 1, which were taken before switching on the lamp and after complete copper photodeposition, suspension color turned from white to light red-brown, whereas pH falls from 5.4 to 3.3.

The process of copper photoreduction and decrease in pH can be ascribed to the reduction of cupric species by photogenerated electrons (r1) and the oxidation of glycerol by photogenerated positive holes (r2):



In order to assess the occurrence of specific side effects that may undermine a correct kinetic evaluation, preliminary experimental runs were performed in the following conditions: (i) in the dark with zero-valent nano-copper P25 catalyst, (ii) under UV-Vis radiation with pristine P25 and glycerol as hole scavengers, and (iii) under UV-Vis radiation in presence of nano- $\text{Cu}_0/\text{P25}$ without glycerol. None of these preliminary tests revealed any nitrate depletion within 5 h of treatment time (data not shown). The results confirmed that (i) both direct nitrate photolysis and nitrate adsorption on the catalyst can be neglected; (ii) in presence of bare TiO_2 , the efficiency of the process to reduce nitrate is negligible; (iii) glycerol acts as a hole scavenger (r2) disfavoring the recombination of photogenerated electron/hole couple.

Figure 2 shows the nitrate conversion degree, the reaction yields for nitrite, ammonia and hydrogen, and the pH variation recorded during 5-h photocatalytic runs.

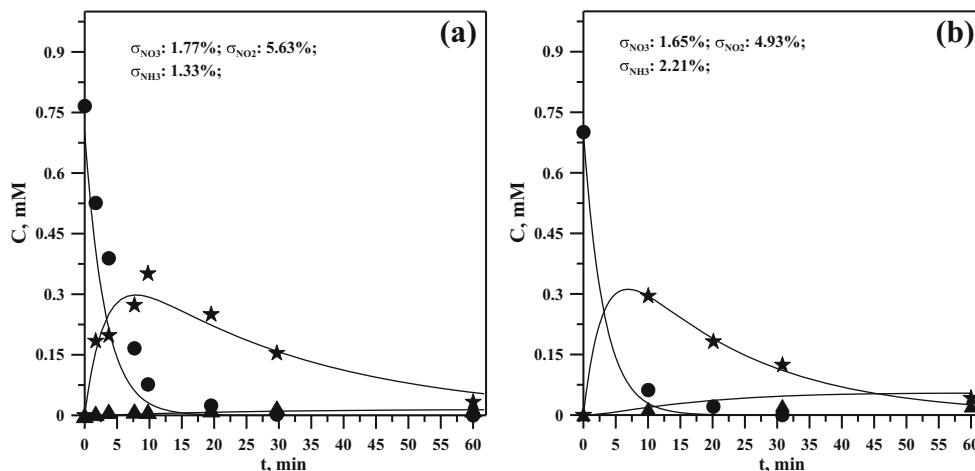
Under the adopted experimental conditions, nitrate ions were totally reduced during the first 30 min of treatments. Longer reaction times were required to remove nitrite ions (120 min) and ammonia (300 min), which were formed as intermediates of the photocatalytic reductive process of nitrate according to the previous literature findings (Ren et al. 2015; Rosca et al. 2009; Soares et al. 2014; Yuzawa et al. 2012).

As soon as a complete removal of nitrate was observed, a hydrogen production was recorded. Hydrogen concentration increased up to a maximum value close to $14 \mu\text{mol/L}$. These observations suggested the hypothesis of competition between

Table 2 Apparent first-order kinetic constant: $[\text{Cu(II)}]_0 = 0.24 \text{ mmol/L}$; $C_{\text{P25}} = 150 \text{ mg/L}$; $[\text{nitrate}]_0 = 50 \text{ mg/L}$

$k_1 \text{ (s}^{-1}\text{)}$	$k_2 \text{ (s}^{-1}\text{)}$	$k_3 \text{ (s}^{-1}\text{)}$	$k_4 \text{ (s}^{-1}\text{)}$	$k_5 \text{ (s}^{-1}\text{)}$
$2.60 \times 10^{-3} \pm 6.51 \times 10^{-4}$	$4.69 \times 10^{-4} \pm 4.44 \times 10^{-6}$	$2.68 \times 10^{-3} \pm 7.46 \times 10^{-5}$	$5.89 \times 10^{-5} \pm 3.33 \times 10^{-6}$	$5.85 \times 10^{-5} \pm 5.00 \times 10^{-7}$

Fig. 5 Comparison between experimental (circles) and calculated (lines) concentrations. Nitrate (black circle), nitrite (black star), and ammonia (black triangle). **a** (Glycerol)₀ = 0.08 mol/L. **b** (Glycerol)₀ = 0.8 mol/L. σ_j percentage standard deviation for *j*-species



nitrate, nitrite, and hydronium reductions by photogenerated electrons (r3 and r4):



In particular, at the beginning of the run, when nitrate concentration is high, nitrate reduction prevails with low or no hydrogen formation. The opposite occurs for higher reaction times.

The increase in pH during the first 60 min of photocatalytic treatment can be related to proton consumption required for reaction r₃. When nitrate and nitrite disappeared, the pH started to decrease due to the occurrence of reaction r₂.

For short treatment times (30 min), the highest conversion degree of nitrate (Fig. 3a) and the lowest nitrite yield (Fig. 3b) were obtained using higher concentrations of glycerol (i.e., 0.8–0.08 mol/L). These starting concentrations of hole scavengers allowed achieving the highest hydrogen productivities (Fig. 3c) and the most relevant pH variations (Fig. 3d). However, for prolonged treatment times (>180 min) the overall conversion degree for both nitrate and nitrite was higher

than 97%, although glycerol concentration was higher than 8.0×10^{-4} mol/L.

In Fig. 4, the logarithm of normalized experimental concentration of nitrate, nitrite, and ammonia removal are, respectively, plotted versus time: a first-order kinetic law provides an appreciable preliminary description of the process kinetics.

The experimental results can be described through the overall reaction:



In reaction (r5), for 1 mol of nitrate reduced to nitrite, 1 mol of alcoholic group is selectively converted into an aldehydic group, thus indicating that the hole scavenger role played by chemical intermediates (i.e., glyceraldehydes, tartronic acid, glyceric acid, etc.) in glycerol oxidation cannot be ruled out.

On the basis of these results and considering the previous literature findings (Ren et al. 2015, Rosca et al. 2009; Soares et al. 2014), a photocatalytic kinetic network of pseudo-first-order reaction for nitrate reduction, nitrite reduction, and ammonia oxidation was proposed (Scheme 1).

As previously stated, nitrate, nitrite, and ammonia concentrations were measured, whereas unidentified nitrogen species, such as N₂ (Zhang et al. 2005; Kominami et al. 2001),

Table 3 Measured concentration of diluted solutions (1/10) during the photocatalytic process. [Cu(II)]₀ = 0.24 mmol/L; C_{in} (P25) = 150 mg/L

Treatment time min	Nitrate		Nitrite		Ammonia		Glycerol mmol/L
	mg/L	mmol/L	mg/L	mmol/L	mg/L	mmol/L	
0	10	0.16	0	0	0	0	0.8
90	0.89	1.43×10^{-2}	0.39	8.48×10^{-3}	5.63×10^{-2}	3.31×10^{-3}	Not measured
180	0.16	2.58×10^{-3}	0.20	4.35×10^{-3}	5.01×10^{-2}	2.95×10^{-3}	Not measured
360	0	0	0	0	3.65×10^{-2}	2.15×10^{-3}	Not measured

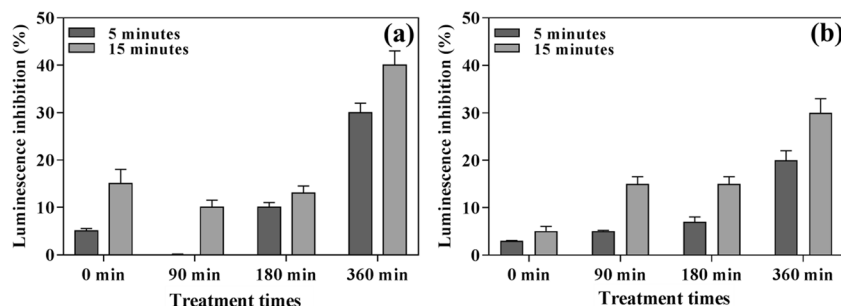


Fig. 6 Luminescence inhibition of *Vibrio fischeri* after 5 and 15 min of exposure. The results are expressed as mean of three replicates \pm standard deviation. **a** Glycerol only (0.8 mmol/L) and its treated solutions. **b** Glycerol (0.8 mmol/L) + nitrate (0.16 mmol/L) and its treated solutions

NO (Montesinos et al. 2015), N_2O , NH_2OH (Goldstein et al. 2016), and N_2H_4 (Yuzawa et al. 2012), were generally indicated as a pseudo-component X .

The kinetic constants of the reaction network proposed were estimated by solving the mass balance differential equations for each species and adopting a least-squares iterative procedure.

Such procedure compares nitrate, nitrite, and ammonia concentrations measured during runs at initial nitrate concentration of 50 mg/L and initial glycerol concentrations in the range 8.0×10^{-1} – 8.0×10^{-3} mol/L, with theoretical values estimated by the Matlab® software. The best estimated values along with their uncertainties are shown in Table 2.

Some comparisons between calculated and measured concentrations for nitrate and nitrite and ammonia are shown in Fig. 5a and b.

Ecotoxicological assessment

An ecotoxicological investigation, using different living organisms (*V. fischeri*, *R. subcapitata*, and *D. magna*), was undertaken on aqueous mixtures of glycerol and nitrate untreated solutions, as well as on samples submitted to the photocatalytic treatment at different irradiation times (0, 90, 180, and 360 min). The measured initial and residual concentrations of

nitrate, nitrite, and ammonia species, after a dilution ratio of 1/10, are reported in Table 3.

Vibrio fischeri

The toxicity values (luminescence inhibition) to *V. fischeri* of untreated samples containing the sole glycerol under all the test regimes ranged from 5 to 15% (Fig. 6). This effect was antagonized by the presence of nitrate with only 5% of toxic effect (untreated sample, 0 min).

Few references can be found in the literature concerning the toxicity of nitrate and glycerol for unicellular species, as the main mechanism of action of glycerol and nitrate is to support cell division in bacteria (Hickey and Martin 2009).

Treated solutions showed a toxic effect which increased with increasing treatment time. After 360 min of photocatalytic treatment, ecotoxicity test of solutions starting from the sole glycerol led to a 40% reduction of luminescence after 15 min of exposure (Fig. 6a), whereas 30% of luminescence inhibition resulted for sample starting from nitrate and glycerol (Fig. 6b).

Raphidocelis subcapitata

The results collected on the ecotoxicity test using *R. subcapitata* alga showed a slight stimulating effect on the algal growth for untreated samples (0 min) (Fig. 7). These data

Fig. 7 Algal (*Raphidocelis subcapitata*) growth inhibition at 72 h of untreated and treated solutions. **a** Glycerol only (0.8 mmol/L). **b** Glycerol (0.8 mmol/L) + nitrate (0.16 mmol/L). Negative values of inhibition indicate stimulation of growth

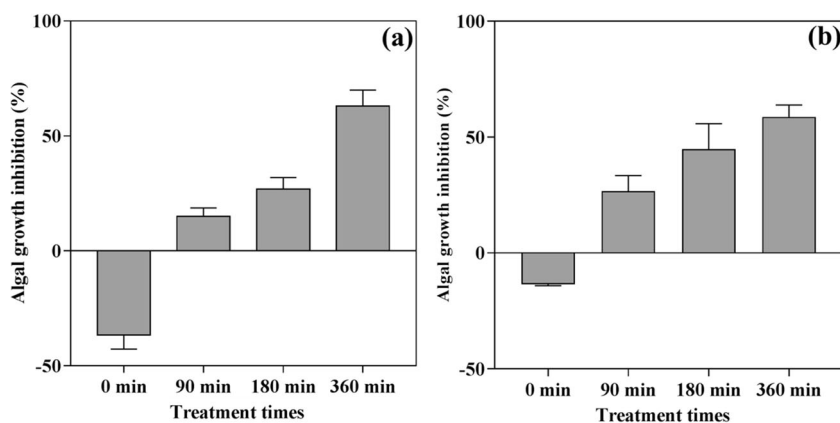
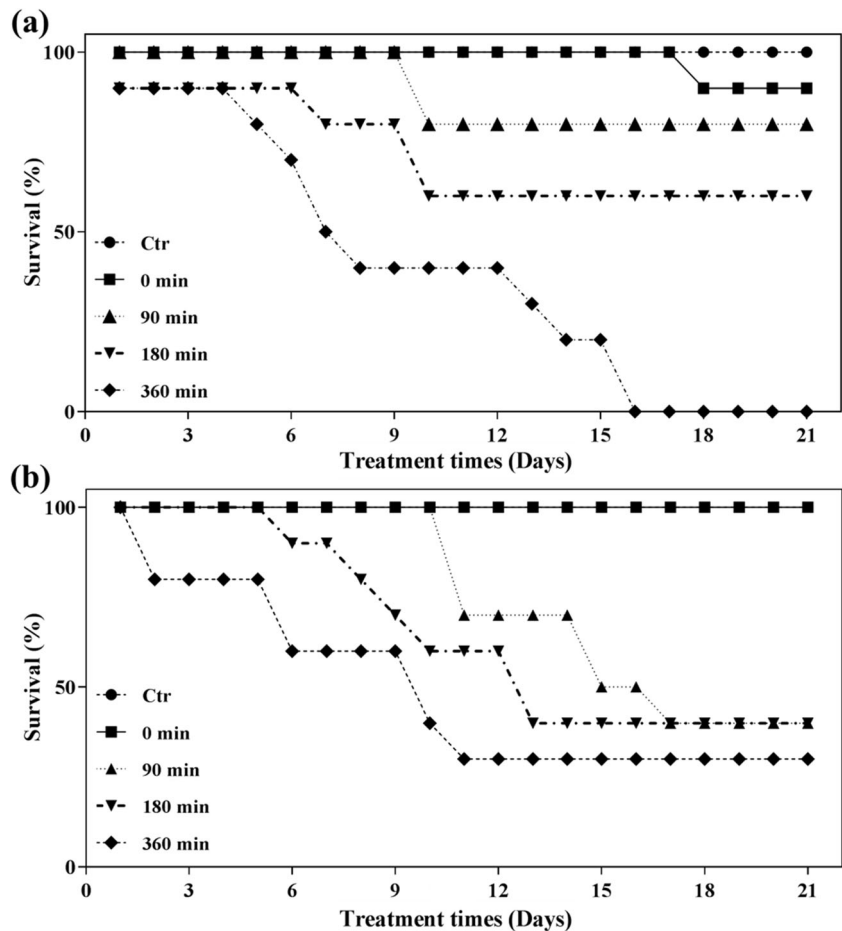


Fig. 8 Survival curves of *D. magna* during the time of exposure (21 days) for untreated and treated solutions. **a** Glycerol only (0.8 mmol/L). **b** Glycerol (0.8 mmol/L) + nitrate (0.16 mmol/L)



are in agreement with the previous literature finding (Wood et al. 1999). On the contrary, an inhibition effect was observed for samples withdrawn after 90, 180, and 360 min of treatment. Similar to the results observed for *V. fischeri*, the ecotoxicity increased with the treatment time.

Daphnia magna

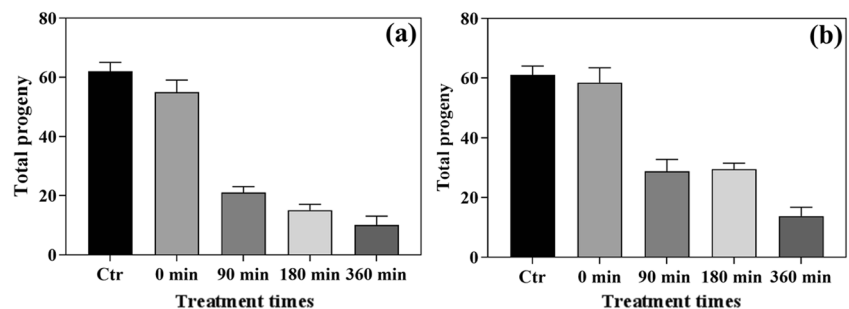
The survival curves for *D. magna* are reported in Fig. 8. The results indicated that the decrease in organism surviving recorded for untreated solutions was not significant with respect to the control data ($p > 0.3$).

The survival degree of cladocerans was markedly lower for treated samples. It was reduced to around 50% after 180 min of treatment. The crustaceans exposed to the aqueous sample collected after 360 min of photocatalytic process showed the highest mortality starting at the sixth day of monitoring with significant statistical differences with control ($\chi^2 = 17.5$, $p < 0.002$).

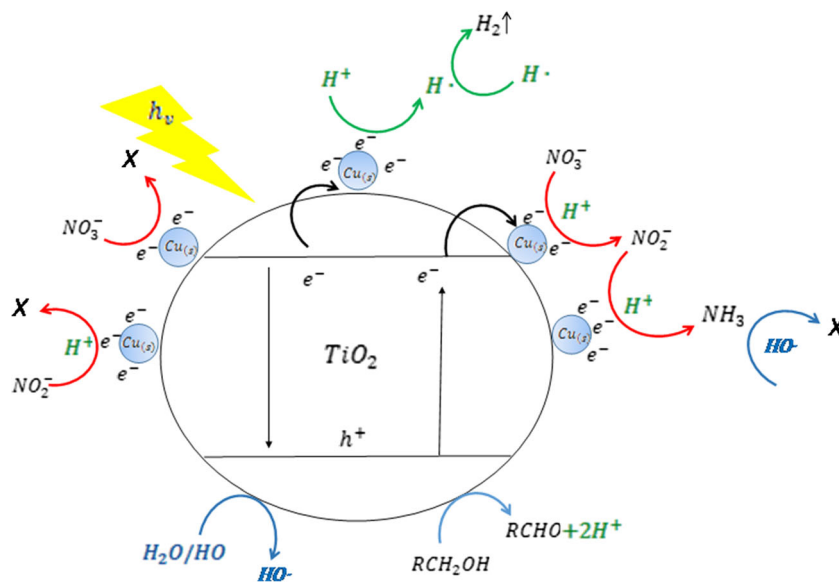
The highest average value of total progeny was recorded for the untreated and treated solutions (Fig. 9).

The lowest value was observed for the sample withdrawn at 360 min (10 and 13.6 neonates resulted from treated solutions starting from glycerol or glycerol + nitrate) against the control group (60.7 neonates per adult). Moreover, the first

Fig. 9 Cumulative number nauplii of *D. magna* after a time of exposure (21 days) for untreated and treated solutions. **a** Glycerol only (0.8 mmol/L). **b** Glycerol (0.8 mmol/L) + nitrate (0.16 mmol/L)



Scheme 2



brood in untreated samples occurred at the tenth day of assay similarly in the control group (9 days). On the other hand, the age of the first reproduction ranged from the 13th to the 15th day in females exposed to the treated samples (data not shown).

The ecotoxicological assessment carried out on multi-trophic species (bacteria, algae, and crustacean) clearly indicated a negative effect of the treated samples, which increased with prolonging the reaction time. Taking into account that both nitrate and nitrite were converted during the process up to a total removal after 360 min of treatment, and that ammonia concentration was more or less constant for the same reaction times (Table 3), it can be inferred that this ecotoxic effect may be mainly ascribed to unknown organic intermediates and by-products formed during the photocatalytic oxidation of the sacrificial agent (glycerol).

Conclusions

A kinetic investigation was undertaken on nitrate and nitrite degradation by means of UV-A-Vis radiation in the presence of zero-valent nano-copper loaded on TiO_2 (P25) and glycerol. The simultaneous production of hydrogen was evaluated at varying initial conditions. Nitrate and photogenerated nitrite were successfully removed. The hole scavenger concentration deeply affects the reaction rate and the hydrogen yield. In particular, hydrogen production increased with increasing initial glycerol concentration, thus highlighting the role of organics in the photocatalytic process. On the basis of the collected data, a simplified kinetic scheme was proposed and the pseudo-first-order kinetic constants were evaluated.

A schematic diagram of the proposed mechanism for nitrate reduction, nitrite reduction, and ammonia oxidation

using zero-valent nano-copper-modified P25 as a photocatalyst and glycerol as a hole scavenger is shown (Scheme 2).

The ecotoxicological assessment pointed out an increase in chronic effects with increasing the treatment time towards the tested organisms, thus indicating an ecotoxic effect of unknown by-products formed during the photocatalytic process. This effect is mostly related to the presence of species deriving from the oxidation of glycerol (used as a hole scavenger). On the other hand, the presence of nitrogen by-products was not related to an increase of the toxicity. The results indicated that copper- TiO_2 (P25) material “in situ” prepared favors the simultaneous photocatalytic hydrogen production and nitrate reduction by promoting the separation of photogenerated charges. However, the possibility of simulating photocatalytic processes in the presence of different hole scavengers could be considered. In addition, further investigations should be performed to (i) identify the main chemical intermediates and by-products and (ii) evaluate the influence of the aqueous matrix (wastewater effluents) and the direct solar irradiation.

References

- Anderson JA (2011) Photocatalytic nitrate reduction over Au/ TiO_2 . *Catal Today* 175:316–321
- Camargo JA, Ward JV (1995) Nitrate toxicity to aquatic life: a proposal of safe concentrations for two species of neararctic freshwater invertebrates. *Chemosphere* 31:3211–3216
- Clarizia L, Di Somma I, Marotta R, Minutolo P, Villamaina R, Andreozzi R (2016b) Photocatalytic reforming of formic acid for hydrogen production in aqueous solutions containing cupric ions and TiO_2 suspended nanoparticles under UV-simulated solar radiation. *Appl Catal A: General* 518:142–149

- Clarizia L, Vitiello G, Luciani G, Di Somma I, Andreozzi R, Marotta R (2016c) In-situ photodeposited nanoCu on TiO₂ as a catalyst for hydrogen production under UV/visible radiation. *Appl Catal A: General* 518:181–188
- Clarizia L, Di Somma I, Onofri L, Andreozzi R, Marotta R *Catalysis Today*. [doi:10.1016/j.cattod.2016.05.053] 2016a.
- Colon G (2016) Towards the hydrogen production by photocatalysis. *Appl Catal A: General* 518:48–59
- Doudrick K, Yang T, Hristovski K, Westerhoff P (2013) Photocatalytic nitrate reduction in water: managing the hole scavenger and reaction by-product selectivity. *Appl Catal B: Environmental* 136–137:40–47
- Gao W, Jin R, Chen J, Guan X, Zeng H, Zhang F, Guan N (2004) Titania-supported bimetallic catalysts for photocatalytic reduction of nitrate. *Catal Today* 90:331–336
- Goldstein S, Behar D, Rajh T, Rabani J (2016) Nitrite reduction to nitrous oxide and ammonia by TiO₂ electrons in a colloid solution via consecutive one-electron transfer reactions. *J Phys Chem A* 120:2307–2312
- Hickey CW, Martin ML (2009) A review of nitrate toxicity to freshwater aquatic species. *Environment Canterbury Report R09/57*.
- ISO 11348-3 (2008) Water quality—determination of the inhibitory effect of water samples on the light emission of *Vibrio fischeri* (luminescent bacteria test)—part 3: method using freeze-dried bacteria
- ISO 8692 (2012) Water quality—fresh water algal growth inhibition test with unicellular green algae
- ISO 6341 (2012) Water quality—determination of the inhibition of the mobility of *Daphnia magna* Straus (Cladocera, Crustacea)—acute toxicity test
- Jin R, Gao W, Chen J, Zeng H, Zhang F, Liu Z, Guan N (2004) Photocatalytic reduction of nitrate ion in drinking water by using metal-loaded MgTiO₃-TiO₂ composite semiconductor catalyst. *J Photochem Photobiol A: Chemistry* 162:585–590
- Jung M, Hart JN, Boensch D, Scott J, Hau Ng Y, Amal R (2016) Hydrogen evolution via glycerol photoreforming over Cu–Pt nanoalloys on TiO₂. *Appl Catal A Gen* 518:221–230
- Kapoor A, Viraraghavan T (1997) Nitrate removal from drinking water—review. *J Environ Eng* 123(4):371–380
- Knobeloch L, Salna B, Hogan A, Postle J, Anderson H (2000) Blue babies and nitrate-contaminated well water. *Environ Health Perspect* 108(7):675–678
- Kominami H, Furusho A, Murakami S, Inoue H, Kera Y, Ohtani B (2001) Effective photocatalytic reduction of nitrate to ammonia in an aqueous suspension of metal-loaded titanium(IV) oxide particles in the presence of oxalic acid. *Catal Letters* 76(1–2):31–34
- Li L, Xu Z, Liu F, Shao Y, Wang J, Wan H, Zheng S (2010) Photocatalytic nitrate reduction over Pt–Cu/TiO₂ catalysts with benzene as hole scavenger. *J Photochem Photobiol A: Chemistry* 212:113–121
- Luiz DB, Andersen SLF, Berger C, Jose HJ, Moreira FPM (2012) Photocatalytic reduction of nitrate ions in water over metal-modified TiO₂. *J Photochem Photobiol A: Chemistry* 246:36–44
- Montesinos VN, Quici N, Destaillets H, Litter MI (2015) Nitric oxide emission during the reductive heterogeneous photocatalysis of aqueous nitrate with TiO₂. *RSC Adv* 5:85319–85322
- Parastar S, Nasser S, Borji HS, Fazlzadeh M, Mahvi HA, Javadi AH, Gholami M (2013) Application of Ag-doped TiO₂ nanoparticle prepared by photodeposition method for nitrate photocatalytic removal from aqueous solutions. *Desalin Water Treat* 51:7137–7144
- Puga AV (2016) Photocatalytic production of hydrogen from biomass-derived feedstocks. *Coord Chem Rev* 315:1–66
- Rao EVSP, Puttanna K (2000) Nitrates, agriculture and environment. *Curr Sci* 79(9):1163–1168
- Ren HT, Jia SY, Zou JJ, Wu SH, Han X (2015) A facile preparation of Ag₂O/P25 photocatalyst for selective reduction of nitrate. *Appl Catal B: Environmental* 176–177:53–61
- Rosca V, Duca M, De Groot MT, Koper MTM (2009) Nitrogen cycle electrocatalysis. *Chem Rev* 109:2209–2244
- Sá J, Aguera CA, Gross S, Anderson JA (2009) Photocatalytic nitrate reduction over metal modified TiO₂. *Appl Catal B: Environmental* 85: 192–200
- Soares OSGP, Pereira MFR, Órfão JJM, Faria JL, Silva CG (2014) Photocatalytic nitrate reduction over Pd–Cu/TiO₂. *Chem Eng J* 251:123–130
- Tan HW, Abdul Aziz AR, Aroua MK (2013) Glycerol production and its applications as a raw material: a review. *Renew Sust Energ Rev* 27: 118–127
- Taylor S, Mehta M, Samokhvalov A (2014) Production of hydrogen by glycerol photoreforming using binary nitrogen-metal-promoted N–M-TiO(2) photocatalysts. *ChemPhysChem* 15:942–949
- Ward MH, DeKok TM, Levallois P, Brender J, Gulis G, Nolan BT, Van Derslice J (2005) Workgroup report: drinking-water nitrate and health—recent findings and research needs. *Environ Health Perspect* 113(11):1607–1614
- Wehbe N, Jaafar M, Guillard C, Herrmann JM, Miachon S, Puzenat E, Guilhaume N (2009) Comparative study of photocatalytic and non-photocatalytic reduction of nitrates in water. *Appl Catal A: General* 368:1–8
- Wood BJB, Grimson PHK, German JB, Turner M (1999) Photoheterotrophy in the production of phytoplankton organisms. *J Biotechnol* 70:175–183
- Yamauchi M, Abe R, Tsukuda T, Kato K, Takata M (2011) Highly selective ammonia synthesis from nitrate with photocatalytically generated hydrogen on CuPd/TiO₂. *J Am Chem Soc* 133:1150–1152
- Yang T, Doudrick K, Westerhoff P (2013) Photocatalytic reduction of nitrate using titanium dioxide for regeneration of ion exchange brine. *Wat Res* 47:1299–1307
- Yoong LS, Chong FK, Dutta BK (2009) Development of copper-doped TiO₂ photocatalyst for hydrogen production under visible light. *Energy* 34:1652–1661
- Yuzawa H, Mori T, Itoh H, Yoshida H (2012) Reaction mechanism of ammonia decomposition to nitrogen and hydrogen over metal loaded titanium oxide photocatalyst. *J Phys Chem C* 116:4126–4136
- Zhang F, Jin R, Chen J, Shao C, Gao W, Li L, Guan N (2005) High photocatalytic activity and selectivity for nitrogen in nitrate reduction on Ag/TiO₂ catalyst with fine silver clusters. *J Catal* 232:424–431